Bioresource Technology, Volume 214, August 2016, Pages 432-440
DOI:10.1016/j.biortech.2016.04.032

Effects of mutation of 2,3-butanediol formation pathway on glycerol metabolism and 1,3-propanediol production by *Klebsiella pneumoniae* J2B

Vinod Kumar [a,c]*, Meetu Durgapal [a]*, Mugesh Sankaranarayanan[a], Ashok Somasundar[a], Chelladurai Rathnasingh[b], HyoHak Song[b], Doyoung Seung[b], Sunghoon Park[a]**

[a] School of Chemical and Biomolecular Engineering, Pusan National University, San 30, Jangeon-dong, Geumjeong-gu, Busan 609-735, Republic of Korea

[b] R&D Center, GS Caltex Corporation, 104-4 Munji-dong, Yusung-gu, Daejeon 305-380, Republic of Korea

[c] Nottingham BBSRC/EPSRC Synthetic Biology Research Centre, Centre for Biomolecular Sciences, University Park, The University of Nottingham, Nottingham NG7 2RD, United Kingdom

*Contributed equally

**Corresponding author

Affiliation: School of Chemical and Biomolecular Engineering, Pusan National University

Mailing Address: School of Chemical and Biomolecular Engineering, Pusan National University, San 30, Jangjeon-dong, Geumjeong-gu, Busan 609-735, Republic of Korea

Phone: +82-51-510-2395

Fax: +82-51-515-2716

E-mail: parksh@pusan.ac.kr

Abstract

The current study investigates the impact of mutation of 2,3-butanediol (BDO) formation pathway on glycerol metabolism and 1,3-propanediol (PDO) production by lactate dehydrogenase deficient mutant of *Klebsiella pneumoniae* J2B . To this end, BDO pathway genes, *budA*, *budB*, *budC* and *budO* (whole-*bud* operon), were deleted from *K. pneumoniae* J2B Δ*ldhA* and the mutants were studied for glycerol metabolism and alcohols (PDO, BDO) production. Δ*budO*-mutant-only could completely abolish BDO production, but with reductions in cell growth and PDO production. By modifying the culture medium, the Δ*budO* mutant could recover its performance on the flask scale. However, in bioreactor experiments, the Δ*budO* mutant accumulated a significant amount of pyruvate (>73 mM) in the late phase and PDO production stopped concomitantly. Glycolytic intermediates of glycerol, especially glyceraldehyde-3-phosphate (G3P) was highly inhibitory to glycerol dehydratase (GDHt); its accumulation, followed by pyruvate accumulation, was assumed to be responsible for the Δ*budO* mutant's low PDO production.

Key words: *Klebsiella pneumoniae* J2B; Glycerol; 1,3-Propanediol; 2,3-Butanediol; Δ*budO* mutant

1. Introduction

1,3-Propanediol (PDO) is an important platform chemical having a wide range of applications in the production of polymers, cosmetics, and lubricants, among others. The most important industrial use of PDO is as a monomer for synthesis of the new polyester polytrimethylene terephthalate (PTT) (Celińska, 2010; Maervoet et al., 2011; Saxena et al., 2009). Many organisms in the *Enterobacteriaceae* family, such as *Klebsiella pneumoniae*, *Klebsiella oxytoca, Citrobacter freundii, Enterobacter aerogenes* and *Enterobacter agglomerans,* naturally produce PDO from glycerol, among which *K. pneumoniae* is the most extensively studied (Celińska, 2010; 2012). *K. pneumoniae* dissimilates glycerol by two parallel "oxidative" and "reductive" pathways (Supplementary Fig. 1). In the oxidative pathway, glycerol is converted to dihydroxyacetone phosphate (DHAP) by a respiratory (aerobic or anaerobic, according to the electron acceptor type) and/or fermentative route, DHAP then being funneled into the glycolytic pathway. In the reductive pathway, glycerol is converted to PDO by a two-step process: first, it is dehydrated to 3-hydroxypropionaldehyde (3-HPA) by the coenzyme B_{12}-dependent glycerol dehydratase (GDHt), which is encoded by *dhaB*; then, 3-HPA, at the expense of NAD(P)H, is reduced to PDO by 1,3-propanediol oxidoreductases (PDORs) such as DhaT (NADH-PDOR) and/or NADPH-dependent oxidoreductase (Celińska, 2012; Kumar et al., 2012; Saxena et al., 2009). The reductive pathway regenerates NAD^+, which enables *K. pneumoniae* to grow on glycerol under limited-O_2 conditions.

During oxidative metabolism of glycerol, *K. pneumoniae* generates a number of metabolites including organic acids (lactic acid, succinic acid, acetic acid, formic acid) and alcohols [2,3-butanediol (BDO), ethanol] (Ashok et al., 2011; Kumar et al., 2013a). These

66 glycerol-metabolic byproducts subdue the glycerol flux to PDO, thereby significantly reducing
67 PDO production yields; additionally, at high concentrations, they are toxic to cell growth and
68 PDO production. Lactic acid, particularly, is a major byproduct (Ashok et al., 2011; Durgapal et
69 al., 2014; Huang et al., 2012), and much research efforts and resources have been devoted to the
70 elimination of its formation (Kumar et al., 2013b; Oh et al., 2012; Xu et al., 2009). Another
71 major byproduct, especially appearing when lactic acid production has been eliminated, is BDO.
72 BDO production reduces PDO yield more significantly than does lactic acid, because synthesis
73 of one molecule of BDO requires two molecules of glycerol. Moreover, due to their similar
74 boiling points, the presence of BDO in the culture broth complicates PDO purification in
75 downstream processing (Anand et al., 2011; Kaur et al., 2012; Zeng and Biebl, 2002). BDO
76 synthesis begins with self-condensation of two molecules of pyruvate to one molecule of C5
77 intermediate α-acetolactate (Supplementary Fig. 1), which is catalyzed by α-acetolactate
78 synthase (ALS, *budB*). In the next step, α-acetolactate is decarboxylated to acetoin (catalyzed by
79 α-acetolactate decarboxylase (ALDC, *budA*)) and then reduced to BDO by 2,3-butanediol
80 dehydrogenase/acetoin reductase (AR, *budC*) using NADH as the reductant. In the presence of
81 oxygen, α-acetolactate is spontaneously decarboxylated to diacetyl, which is then reduced to
82 acetoin by the action of diacetyl reductase, and acetoin in turn is reduced to BDO. When diacetyl
83 is converted to acetoin or acetoin is converted to BDO, one NADH, at each step, is required
84 (Celińska and Grazek, 2009; Ji et al., 2011). The genes coding for the three enzymes in the BDO-
85 producing branch are located in one operon (*budO*) in the order *budA* (ALDC), *budB* (ALS) and
86 *budC* (AR).

87 The current study investigated the role of the three enzymes of the BDO synthetic
88 pathway in cell growth, glycerol metabolism and BDO production under different aeration

89 conditions. Also, the possibility of producing PDO at an economically feasible level without
90 BDO production was explored. The newly isolated *K. pneumoniae* J2B (KCCM11213P) strain
91 was used, as it does not produce pathogenic and sticky lipopolysaccharides (Arasu et al., 2011),
92 and also because it has better sedimentation properties and a higher sensitivity to antibiotics than
93 other well-studied *K. pneumoniae* such as the DSMZ2026 strain. Using *K. pneumoniae* J2B
94 Δ*ldhA* as the base strain, four mutant strains (Δ*budA*, Δ*budB*, Δ*budC* and Δ*budO*) were
95 developed and their performances studied by shake-flask and bioreactor experiments.

96 **2. Materials and methods**

97 **2.1 Materials**

98 A genomic DNA isolation kit and pGEM-T vector was purchased from Promega
99 (Madison, WI, USA). High-fidelity *pfx* polymerase was acquired from Invitrogen (Seoul, Korea).
100 Restriction DNA-modifying enzymes were obtained from New England Bio-Labs (Beverly, MA,
101 USA). The miniprep and DNA gel extraction kits were purchased from Qiagen (Mannheim,
102 Germany). The primers were synthesized by Cosmotech Co. Ltd. (Seoul Korea).Yeast extract
103 (Cat. 212750) was obtained from Difco (Becton Dickinson; Franklin Lakes, NJ, USA). Glycerol
104 and all other chemicals and enzymes (unless indicated otherwise) were purchased from Sigma-
105 Aldrich (St. Louis, MO, USA).

106 **2.2 Construction of plasmids and mutant strains**

107 All of the strains, plasmids and primers are listed in Table 1. For the design of the four
108 mutant strains of *K. pneumoniae* J2B (Δ*budA*, Δ*budB*, Δ*budC* and Δ*budO*), an in-frame tagged
109 deletion approach was employed according to a slightly modified version of the method

introduced by Link et al. (1997). Briefly, PCR amplification of ~500 bp of the upstream (fragment A) and ~500 bp of the downstream (fragment B) regions of the above-noted genes was performed using the primers listed in Table 1. In the next step, the two amplified fragments A and B were ligated using overlapping PCR methods to synthesize the engineered fragment AB, which subsequently was cloned into the pGEMT vector. After confirming this sequence, the engineered fragment AB was sub-cloned into the pKOV vector between the restriction sites (shown in Table 1). These plasmids were used to knock out, by homologous recombination, the target genes from the chromosomal DNA of *K. pneumoniae* J2B Δ*ldhA*. The mutant strains were screened using PCR and confirmed by sequencing. The developed mutant strains of *K. pneumoniae* J2B Δ*ldhA*, Δ*ldhA*Δ*budA*, Δ*ldhA*Δ*budB*, Δ*ldhA*Δ*budC* and Δ*ldhA*Δ*budO*, were designated KpΔ*budA*, KpΔ*budB*, KpΔ*budC* and KpΔ*budO*, respectively. *K. pneumoniae* J2B Δ*ldhA* was designated as the *K. pneumoniae* control (Kp control).

2.3 Shake-flask cultivation

Shake-flask experiments were carried out at 37°C with an initial pH of 7. Different strains used in gene-deletion studies were cultured in Luria-Bertani medium (LB medium) containing yeast extract (5 g/L), NaCl (10 g/L), and tryptone (10 g/L). For shake flask production experiments, a primary inoculum was prepared by culturing cells in LB medium from agar plates for 8 h. From the primary inoculum, the cells were transferred to fresh LB medium for 2 h in order to harvest active cells at the mid-log phase. The primary and the secondary inoculum cultures were grown under the same conditions (working volume: 50 mL in 250 mL Erlenmeyer flask; agitation speed: 200 rpm; initial pH: 7.0, temperature: 37°C). The cell OD_{600} at the end of pre-cultures I and II were in the 5.0 - 6.0 and 1.5 - 2.0 ranges, respectively. The

starting OD_{600} in all of the experiments was 0.1 - 0.2, and so the inoculum volume was dependent on the final OD_{600} achieved at the end of each stage. The main cultivation of the designed mutant strains of *K. pneumoniae* J2B (Kp control, KpΔ*budA*, KpΔ*budB*, KpΔ*budC* and KpΔ*budO*) was conducted in 250 mL flasks containing a medium of the following composition: glycerol-20 g/L (220 mM), yeast extract-1.0 g/L, NH_2SO_4-2.0 g/L, $MgSO_4 \cdot 7H_2O$-0.2 g/L, $CaCl_2.2H_2O$-0.02 g/L, K_2HPO_4-3.4 g/L, KH_2PO_4-1.3 g/L; Fe solution-1 mL/L, and trace-element solution-1 mL/L (Oh et al., 2012).

Shake-flask cultivation of the different mutant strains was performed under various aeration conditions: aerobic, microaerobic, and anaerobic. In the aerobic and microaerobic cultures, the flasks were plugged with an oxygen-permeable cotton stopper; in the anaerobic cultures, the flasks were closed with a screw cap, and the flask head space was replaced with argon gas prior to cultivation. The working volumes under aerobic, microaerobic, and anaerobic conditions were 25, 100 and 50 mL, respectively. The agitation speed under the aerobic condition was 250 rpm, and under both the microaerobic and anaerobic conditions, 100 rpm. The culture medium was supplemented with different components in order to investigate their effects on cell metabolism and PDO production. The KpΔ*budA* and KpΔ*budO* strains were supplemented with two different concentrations of branched-chain amino acids (leucine, isoleucine, and valine) (1.0 and 2.0 mM) as well as complex nitrogen sources (yeast extract-1.0 g/L, peptone-2.5 g/L, beef extract-2.5 g/L, yeast extract-2.5g/L, peptone-5.0 g/L, beef extract-5.0 g/L). The shake-flask cultivation of KpΔ*budO* was additionally supplemented with exogenous additions of BDO (25 mM) and $NaHCO_3$ (50 mM).

2.4 Bioreactor cultivation

The bioreactor experiments were carried out in a 1.5 L jar bioreactor (KO Biotech, Korea) containing a 1.0 L medium of the same composition as in the shake-flask cultivation (see above). The inoculum culture was prepared in the same way as described for the flask experiment. The pH, temperature, stirrer speed and aeration rate in the bioreactor experiments were maintained at 6.8, 37°C, 250 rpm and 0.5 vvm, respectively, unless specified otherwise. The pH was maintained by addition 5 N NaOH. Fed-batch experiments were performed using KpΔ*budO* with a feeding solution of glycerol (1,000 g/L; 10.9 M) and yeast extract (25 g/L). In one run, carbon dioxide (CO_2) was continuously flushed at an aeration rate of 0.05 vvm, and in another run, $NaHCO_3$ (100 mM) was added to the culture medium.

2.5 Glycerol dehydratase (DhaB) activity and inhibition by glycerol metabolites

K. pneumoniae cells grown in LB medium were induced and harvested 3 h from the time of induction. The harvested cells were lysed anaerobically using a bead beater and subjected to a DhaB-activity assay inside an anaerobic chamber. An appropriate amount of cell lysate was pre-incubated with 10 mM of potassium phosphate buffer (pH 7), purified KGSADH and 40 mM 1,2-PDO at 37°C for 3 min. The reaction was initiated by adding 15 µM coenzyme-B_{12}, 1.5 mM ATP, 3 mM $MgCl_2$ and 2 mM NAD^+ to the reaction mixture for a total volume of 2 mL. In this mixture, 1,2-PDO acts as a substrate for DhaB protein and is converted to propionaldehyde, which, in sequence, is converted to propionic acid by the action of coupling-enzyme KGSADH. The activity of KGSADH was evaluated by measuring the reduction of NAD^+ to NADH at 340 nm. The amount of NADH formed was determined using an extinction coefficient of 6.22 mM^{-1} cm^{-1}. One unit of enzymatic activity was defined as the amount of

enzyme required to form 1 μmol of propionaldehyde per minute. The metabolites pyruvate, DHAP, MG, G3P and DHA were added to the enzymatic reaction mixture in different concentrations (0.5, 1, 2, 5 and 10 mM, respectively) in order to study their individual inhibitory effects.

2.6 Analytical methods

Cell density was measured in a 10-mm-path-length cuvette using a double-beam spectrophotometer (Lambda 20, PerkinElmer; Norwalk, CT, USA). One unit of absorbance at 600 nm (OD_{600}) corresponded to 0.31 g dried cell mass per liter. The concentrations of glycerol and of the other metabolites were determined by HPLC using a slightly modified version developed by Raj et al. (2008). Briefly, the supernatants, obtained by centrifuging the culture samples at 10,000 ×g for 10 min, were filtered through a Tuffryn membrane (Acrodisc, Pall Life Sciences, USA) and eluted through a 300 ×7.8 mm Aminex HPX-87H (Bio-Rad, USA) column at 65°C. The mobile phase and flow rate were 2.5 mM H_2SO_4 and 0.5 mL/min, respectively. All of the experiments were carried out at least three times to ensure reproducibility. The data reported are the averaged values for three independent measurements; the standard deviation was less than 10% unless otherwise indicated.

3. Results and discussion

3.1 Metabolic changes in Kp control, Kp∆*budA*, Kp∆*budB*, Kp∆*budC* and Kp∆*budO* under different aeration conditions during flask cultivation

Five mutant strains, one base strain (Kp control) and four BDO-pathway mutant strains (Kp∆*budA*, Kp∆*budB*, Kp∆*budC* and Kp∆*budO*) were developed and cultured under three

197 different aeration conditions (aerobic, microaerobic and anaerobic) (Table 2). Cell growth,
198 glycerol consumption and PDO production significantly varied depending on the genes disrupted
199 and aeration conditions adopted for cultivation. Under aerobic condition, the growths of
200 Kp∆*budB* and Kp∆*budC* (OD_{600}, 7-8) were similar to that of the Kp control (OD_{600}, 7.6) whereas
201 those of Kp∆*budA* and Kp∆*budO* (OD_{600}, 4-5) were lower. Similarly, glycerol consumption was
202 high in Kp∆*budB* and Kp∆*budC* (~200 mM) but low in Kp∆*budA* and Kp∆*budO* (<70 mM).
203 PDO production was generally low under the aerobic conditions, due mainly to insufficient
204 production of coenzyme B_{12}. Among the mutant strains, Kp∆*budB* and Kp∆*budC* (38-41 mM)
205 produced much higher PDO than did Kp∆*budA* or Kp∆*budO* (2-6 mM); but none of the mutants
206 showed higher PDO production than that of the Kp control (44.7 mM) under the aerobic
207 conditions. BDO production decreased when the enzyme(s) of the BDO pathway were disrupted,
208 but varyingly; Kp∆*budB* and Kp∆*budC* showed a small decrease, while Kp∆*budA* manifested a
209 significant drop. It was noted that ∆*budO*-only completely abolished BDO production. The low
210 impacts of ∆*budB* and ∆*budC* were attributed to the presence (and active expression) of the
211 isozymes of ALS (encoded by *budB*) and AR (encoded by *budC*). Recently it was reported that
212 AR can convert 3-hydroxypropionaldehyde to 1,3-PDO, similar to 3-hydroxypropionaldehyde-
213 specific oxidoreductase, DhaT (Wang et al., 2014). Wu et al. (2013), moreover, earlier reported
214 the presence of several genes having similar sequences to that of *budC*. The low cell growth and
215 glycerol consumption in Kp∆*budA* indicates that *budA* does not have isozyme(s), and further,
216 that accumulation of the substrate of *budA*, α-acetolactate, is highly toxic to cells. The detour
217 route for the conversion of α-acetolactate to acetoin via diacetyl can compensate for the lack of
218 *budA* isozymes, but its efficiency seems to be low. The similar behaviors of Kp∆*budA* and
219 Kp∆*budO* with respect to cell growth, glycerol consumption and PDO production, among others,

220 strongly suggest that, under aerobic conditions, Δ*budA* is the most influential of all of the
221 mutations in the BDO operon.

222 Under the anaerobic condition, cell growth decreased while PDO production increased.
223 Kp*ΔbudB* and Kp*ΔbudC* (final OD_{600}, 3-4) showed a higher cell density than Kp*ΔbudA* or
224 Kp*ΔbudO* (final OD_{600}, ~1.9). Surprisingly, the Kp control, similarly to the latter two mutants,
225 showed low cell growth (final OD_{600}, ~1.9). Glycerol consumption and PDO production were
226 high in Kp*ΔbudB* and Kp*ΔbudC*, and low in Kp*ΔbudA* and Kp*ΔbudO*, in comparison to Kp
227 control. As was the case under the aerobic conditions, Kp*ΔbudA* and Kp*ΔbudO* showed similar
228 behaviors in terms of cell growth, glycerol consumption, and production of PDO and other
229 metabolites; this suggests, again, that *budA* deletion has a higher impact on the BDO pathway
230 than either *budB* or *budC* deletion. It should be noted, too, that whereas Kp*ΔbudB* and Kp*ΔbudC*
231 showed similar cell growth and PDO production, the metabolite production profiles were
232 significantly different: Kp*ΔbudB* produced much acetate and little ethanol, while Kp*ΔbudC*
233 produced much ethanol and little acetate. Also, whereas Kp*ΔbudB* did not produce BDO,
234 Kp*ΔbudC* produced a significant amount of it, even more than the Kp control. It is not clear why
235 Kp*ΔbudB* and Kp*ΔbudC* show such different behaviors, though we speculate that it must be
236 closely related to NADH balance. As indicated in supplementary Fig. 1, BDO production
237 generates, from the two moles of pyruvate with consumption of one mole of NADH and
238 unutilized NADH molecules may be consumed in the production of ethanol (i.e., in Kp*ΔbudC*).
239 If, as in the case of Kp*ΔbudB*, BDO is not produced, no excessive NADH are generated, and
240 thus, acetate production is the right venue. In addition, acetate production yields ATP, which
241 seems always to be beneficial to cells. This NADH effect is observed also under aerobic
242 conditions, though not as significantly. We assume that, under aerobic conditions, maintenance of

the redox balance can be managed rather easily by active operation of the electron transport chain. And in fact, under microaerobic conditions, cell growth, glycerol consumption and PDO production were quite similar to those under anaerobic conditions, as were the metabolite production profiles. Once again, these results indicate that, among the three genes, *budA* deletion has the greatest impact on glycerol metabolism.

BDO production, meanwhile, was suppressed by mutations in the BDO pathway, though its complete elimination was observed only in KpΔ*budO*. In most of the strains tested, acetate and ethanol were produced as major byproducts, towards which, additional carbon flux was diverted upon suppression of the BDO pathway. In some cases, especially with KpΔ*budB* and KpΔ*budO*, substantial pyruvate excretion was observed; indeed, with KpΔ*budO,* a significant pH drop (below 5.0) also was noticed. Such pyruvate excretion and pH loss in KpΔ*budO* suggests that the complete elimination of the BDO pathway in the *ldhA*$^-$ background causes heavy metabolic traffic at the pyruvate node.

3.2 Flask culture of KpΔ*budO* with supplementation of amino acids, $NaHCO_3$ and/or BDO

Among the four mutant strains, only KpΔ*budO* could produce PDO without BDO accumulation. However, after elimination of the whole-*bud* operon, glycerol consumption and PDO production were sharply diminished. In order to explore the reasons for this as well as the possibility of PDO production without BDO, optimization of KpΔ*budO* culture conditions was performed. All of the experiments were carried out under the microaerobic condition, as these, among the three aeration conditions, had proved the most conducive to cell growth and PDO production. First, the effect of complex nitrogen was studied. Branched-chain amino acids (leucine, isoleucine and valine) or larger amounts of complex nitrogen sources (yeast extract,

beef extract, and peptone) were added to the culture medium. It was hypothesized that elimination of the *bud* operon might curtail the availability of the three essential branched-chain amino acids, due to the lack of their precursor, α-acetolactate, the first intermediate of the BDO pathway (see supplementary Fig. 1). The branched-chain amino acids were added to the culture medium at two different concentrations (1 and 2 mM each), as were the mixtures of complex nitrogen sources (1 g/L yeast extract, 2.5 g/L peptone and 2.5 g/L beef extract; 2.5 g/L yeast extract, 5 g/L peptone and 5 g/L beef extract) (data not shown). However, no improvement in glycerol consumption or PDO production was noted for any of the cultures.

Next, the effects of higher phosphate concentration (100 mM) and the addition of BDO and/or $NaHCO_3$ were studied (Fig. 1). The testing of the high phosphate concentration was carried out owing to the precipitous pH drop (below 5.0) that had been observed in the experiments where 29 mM of potassium phosphate was used (see Table 1 for data). As for BDO supplementation, we sought to determine if BDO itself, the final product of the BDO pathway, has a physiological role (its lack had hampered glycerol consumption and PDO production). In the same context, we hypothesized that the lack of CO_2, which is generated at 2 moles per mole of BDO (see supplementary Fig. 1), can hamper the performance of Kp∆*budO*. In the preliminary results, the increase in the buffering capacity of the culture medium, from 29 to 100 mM, greatly improved glycerol consumption and PDO production (Figs. 1C and 1D): 91.1 mM PDO in a significantly enhanced yield (0.67 mol PDO/mol glycerol) was produced from 135.8 mM glycerol in 12 h. However, the pH nonetheless decreased below 5.3 after 9 h, and a substantial amount of glycerol was left unused. Significantly, the addition of BDO (25 mM) to the high-buffer culture medium barely affected the performance of the strain (Figs. 1E and 1F). The addition of $NaHCO_3$

288 (50 mM), on the other hand, further improved glycerol consumption and PDO production (Figs.
289 1G and 1H): more than 90% of glycerol was consumed in 9 h, and cell growth (3.0 at OD_{600})
290 along with the PDO titer (112 mM) were enhanced by 45.4 and 22.5%, respectively, relative to
291 the case without $NaHCO_3$. Significantly too, when BDO was additionally supplemented to the
292 $NaHCO_3$-containing medium (Figs. 1I and 1J), no further improvement in PDO production was
293 observed. Sodium bicarbonate ($NaHCO_3$) is a source of CO_2, but it can also counteract pH drop
294 caused by generation of various acids. When $NaHCO_3$ was added, the final pH increased to ~5.8
295 (Figs. 1G and 1I) from ~5.3 (Figs. 1C and 1E). The production of metabolites, meanwhile, varied
296 significantly with the culture conditions (Figs. 1B, 1D, 1F, 1H and 1J). Acetate, pyruvate and
297 formate were the major byproducts, with ethanol, lactate and succinate as the minor ones (under
298 10 mM). When $NaHCO_3$ was added, production of acetate (~40 mM) and formate (~27 mM) was
299 greatly increased, whereas pyruvate excretion was greatly reduced. This suggests that the
300 addition of $NaHCO_3$ and/or the increase of culture pH stimulates pyruvate-formate-lyase (PFL),
301 which converts pyruvate to acetyl-CoA and formate, thereby reducing pyruvate accumulation. As
302 for succinate, its production was slightly increased, suggesting that carboxylation of pyruvate to
303 oxaloacetate also was stimulated. Overall, these results indicate that, in the KpΔ*budO* mutant
304 where both the lactic acid and BDO production pathways were eliminated, excessive production
305 of acids (especially the accumulation of pyruvate) and/or subsequent pH drop could be the
306 principal cause of the reduction of PDO production and cell growth, and that their negative
307 impact can be greatly alleviated by increasing medium buffering capacity and/or the addition of
308 $NaHCO_3$ to the culture medium. It should also be noted that KpΔ*budO* cultured under
309 microaerobic and modified conditions exhibited a similar performance (in terms of cell growth,

glycerol consumption, PDO production, final pH, production of acetate and ethanol, etc.) to that of Kp∆*budB* cultured under anaerobic and non-modified conditions.

3.3 Batch bioreactor experiments on Kp∆*budO* with $NaHCO_3$ or continuous CO_2 supply

The effects of CO_2 and $NaHCO_3$ on Kp∆*budO* performance was further studied using pH-controlled bioreactors in a batch mode (Fig. 2). Carbon dioxide was added in the form of $NaHCO_3$ (100 mM) or by continuous sparging of CO_2 gas at 0.05 vvm. The pH was maintained at 7.0 and the initial glycerol concentration was set to 600 mM. Despite the pH maintenance, Kp∆*budO* exhibited a performance much inferior to the Kp control. When $NaHCO_3$ was added, some improvement in cell growth and PDO production was noticed, but not to the level by the Kp control. Specifically, whereas the Kp control produced ~305 mM PDO, Kp∆*budO* with $NaHCO_3$ produced only 265 mM. In the case of the continuous sparging of CO_2 (Fig. 2E), PDO production and cell growth were even lower than in the case without CO_2 (Fig. 2C), suggesting that excessive CO_2 is inhibitory. Cell growth and glycerol consumption also were lower in Kp∆*budO*. Overall, these results indicate that the negative impact of the deletion of the *bud* operon, cannot be removed by simple optimization of culture conditions at flask level. These bioreactor results also suggest that the improvement of the performance of Kp∆*budO* (shown in Fig. 1) was mostly owed to the increase of the culture pH to a more neutral level.

The major end products of glycerol metabolism in *K. pneumonia* under limited-aeration conditions are lactic acid and BDO (Durgapal et al., 2014). When lactic acid production is blocked, more BDO is produced, and vice versa. If both BDO and lactic acid production are blocked at the same time, other metabolites such as ethanol, acetate, formate, hydrogen, succinate, and others will be produced at higher concentrations to keep the carbon flow at the pyruvate node (see supplementary Fig. 1). Otherwise, due to metabolic traffic at the pyruvate

node, glycerol metabolism through the oxidative pathway is terminated, which seemingly was the case with the current KpΔ*budO*. There are three strategies for dealing with the carbon traffic problem at the pyruvate node of *K. pneumonia* that lacks both *ldhA* and *budO*. First, the consumption of pyruvate through the TCA cycle can be accelerated. Among the advantages of this strategy is improved cell growth and viability, and enhanced the NADH supply for PDO production. On the other hand, the glycerol-to-PDO yield can be reduced if carbon is mainly used for cell growth. The second strategy for dealing with the carbon traffic problem at the pyruvate node is suppression of pyruvate generation by reduction of glycerol consumption through the oxidative pathways at the glycerol node (by perturbing the expressions of *glpK*, *gldA* and/or *dhaD*; see supplementary Fig. 1). The advantage and disadvantage of the second strategy are exactly the opposite of those indicated for the first strategy. Furthermore, a lowered NADH production rate can lead to a greatly reduced PDO production rate. The third and most desirable strategy is to accelerate the PDO production (reductive) pathway relative to the oxidative pathway at the glycerol node. Zheng et al. (2006) attempted overexpression of *dhaB* to enhance the reductive pathway in a wild-type strain of *K. pneumonia* which resulted in accumulation of toxic 3-HPA; it did not improve PDO production (though it should be noted that minimization of BDO production was not their goal). No report on *dhaB* and *dhaT* expression enhancement in the background of Δ*ldhA* and Δ*budO* has yet been published.

One additional interesting feature of the present bioreactor experiments with KpΔ*budO* was the re-appearance of lactic acid, which had not been observed in the flask experiments. We speculated that activation of the pathway via methylglyoxal was responsible for this (see supplementary Fig. 1). To prove that hypothesis, the *mgsA* deletion mutant *K. pneumonia* J2B

355 Δ*ldhA*Δ*budO*Δ*mgsA* was developed and tested (data not shown). The results showed that even
356 though no detectable lactic acid was produced, PDO production was not improved.

357 **3.4 Fed-batch bioreactor experiments on KpΔ*budO***

358 Among the above-suggested strategies for alleviation of the carbon traffic at the
359 pyruvate node, the first, which is to say, improvement of TCA-cycle throughput was briefly
360 examined. This goal can be accomplished by increasing aeration and/or supplying additional
361 nitrogen. First, increased yeast-extract concentration (initial concentration: 5 g/L) was explored
362 (Fig. 3). The air-flow rate was set at 0.5 vvm. For comparison, the same experiments but with
363 1 g/L yeast extract were also performed for both the Kp control and KpΔ*budO*. The PDO
364 production of the Kp control with 1 g/L yeast extract was 752.9 mM at 36 h; under the same
365 conditions, KpΔ*bud*O produced only ~410 mM PDO. For both strains, the initial (to 6 h) cell
366 growth and PDO production, ~ 5 OD and 130 ~ 150 mM, respectively, were similar; thereafter
367 however, KpΔ*bud*O showed a performance significantly inferior to that of the Kp control.
368 Moreover, from 6 h, KpΔ*bud*O started to accumulate pyruvate and lactate, as in the batch
369 bioreactor experiments. When the initial yeast-extract concentration was elevated to 5 g/L (Fig.
370 3E and 3F), the cell growth rate and glycerol consumption were greatly accelerated, and the
371 maximum cell density (OD_{600}-12) reached a significantly higher level at ~15 h. The final PDO
372 titer also was considerably improved, to 512 mM, at 36 h. However, the level did not match that
373 of the Kp control, as the PDO production rate had declined significantly after 12 h.
374 Interestingly, the two strains' molar PDO yields with glycerol were comparable (Kp control,
375 0.43; KpΔ*bud*O, 0.46).

376 The metabolite profiles of the two strains are compared in Table 3. The cultivation phase
377 was divided into two phases according to the cell-growth pattern and metabolite production.

The carbon recoveries in each phase were higher than 95% when the yeast extract was 1 g/L, but were reduced to ~85% when the yeast extract was elevated to 5 g/L. The reason for this is not clear. With Kp∆*bud*O, glycerol assimilation in the second phase was greatly reduced relative to that in the first phase. With the Kp control, a large amount of BDO, ~274 mM, was produced in 36 h. In Kp∆*bud*O, the glycerol carbon that had been used for BDO formation in the Kp control seemed to be diverted to a variety of metabolites, especially formate, acetate, pyruvate, lactate and ethanol. However, the total amount diverted to these metabolites was far less than that of BDO in the Kp control, indicating that glycerol assimilation and its metabolism was significantly reduced in Kp∆*bud*O. It was also noted that, as in the batch experiments, Kp∆*bud*O produced pyruvate and lactate at high concentrations. The high accumulation of pyruvate, even with a high concentration of yeast extract, indicated that the strategy to alleviate the carbon traffic at the pyruvate node by supplementing additional, readily-usable nitrogen and stimulating the TCA cycle was not successful, especially in the later phase of the bioreactor experiment.

In order to stimulate TCA throughput, another set of bioreactor experiments with an increased aeration rate (to 1 vvm) were performed (data not shown). Cell growth and glycerol consumption were enhanced in all three cases (Kp control with 1 g/L yeast extract; Kp∆*budO* with 1 g/L yeast extract; Kp∆*budO* 5 g/L yeast extract), but PDO production was reduced by ~15%. Also, PDO production began at ~6 h, about 3 h later than in the former, 0.5 vvm-aeration-rate case, probably due to lowered or delayed synthesis of coenzyme B_{12}. With Kp∆*budO*, metabolic traffic at the pyruvate node was not alleviated, >50 mM pyruvate having been accumulated. Intermittent feedings of yeast extract in the later phase did not improve glycerol consumption and/or PDO production. Again, these results show that carbon traffic at

401 the pyruvate node could not be lessened by increasing aeration and/or addition of a rich nitrogen
402 source.

403 It has been reported that *K. pneumoniae* has an inefficient or incomplete TCA cycle,
404 unlike other, similar enterobacter sp. such as *E. coli* (Cabelli, 1955). In that study, the growth
405 with fumarate or succinate as the sole carbon source required a much longer lag period than that
406 with TCA intermediates including malate, oxaloacetate, citrate and others, and it was suggested
407 that fumarate does not go to malate. According to our preliminary studies, transcription of some
408 enzymes (e.g., *fumA* and *sdhA*) was low, as were their enzymatic activities, especially under the
409 anaerobic condition. If the TCA cycle does not operate properly, pyruvate utilization cannot be
410 efficient and/or stimulation of TCA-cycle throughput becomes highly challenging. This suggests
411 that in the context of the production of PDO without BDO, *K. pneumoniae* has a serious
412 limitation as a microbial cell factory. Additional studies on the TCA cycle of *K. pneumoniae* are
413 in progress.

414 **3.5 Effects of glycerol carbon metabolites on glycerol dehydratase (DhaB) activity**

415 The results obtained thus far indicate that the metabolic traffic at the pyruvate node is
416 critical to glycerol metabolism in KpΔ*budO*. Accumulation of pyruvate causes that of other
417 glycolytic intermediates such as dihydroxyacetone (DHA), dihydroxyacetone phosphate
418 (DHAP), methylglyoxyl (MG) and glyceraldehyde-3-phosphate (G3P), and threatens to
419 terminate glycerol assimilation through the oxidative pathway. Further, if any of these
420 metabolites specifically inhibit the activity of glycerol dehydratase (DhaB) (see supplementary
421 data Fig. 1), the conversion of glycerol to PDO also is greatly reduced. Therefore, the effect of
422 glycolytic intermediates on DhaB activity was studied using crude cell extract expressing DhaB

423 at a high level (Fig. 4). Among the metabolites tested, G3P was the most highly inhibitory: at 1
424 mM, DhaB activity was completely eliminated. Other metabolites such as pyruvate, MG and
425 DHAP also showed some inhibition, but much less significantly than G3P. DHA was not
426 inhibitory up to 10 mM. These results suggest that G3P followed by pyruvate accumulation
427 greatly decreases reductive flux in addition to oxidative flux, which eventually halts glycerol
428 consumption.

429 **4. Conclusion**

430 The current study investigated the effects of the deletion of the BDO pathway on glycerol
431 metabolism and PDO production by *K. pneumoniae* J2B Δ*ldhA*. The deletion of *budO* (whole-
432 *bud* operon) could completely eliminate BDO production, but this triggered heavy carbon-
433 metabolic traffic at the pyruvate node. Glycerol dehydratase, which converts glycerol to 3-HPA,
434 was specifically inhibited by G3P which should accumulate along with pyruvate. It is suggested
435 that pyruvate accumulation should be strictly prevented during PDO production by carefully
436 decreasing oxidative flux and/or increasing reductive flux.

437 **Acknowledgements**

438 This study was supported financially by the Korean Ministry of Education, Science, and
439 Technology through the Advanced Biomass R&D Center (ABC; Grant No. 2010-0029799),
440 KAIST, Korea. The authors are also grateful for the financial assistance provided by the BK21
441 Plus Program for Advanced Chemical Technology at Pusan National University.

References

1. Anand, P., Saxena, R.K., Marwah, R.G., 2011. A novel downstream process for 1,3-propanediol from glycerol-based fermentation. Appl. Microbiol. Biotechnol. **90**(4), 1267-1276.

2. Arasu, M., Kumar, V., Ashok, S., Song, H., Rathnasingh, C., Lee, H., Seung, D., Park, S., 2011. Isolation and characterization of the new *Klebsiella pneumoniae* J2B strain showing improved growth characteristics with reduced lipopolysaccharide formation. Biotechnol. Bioprocess Eng. **16**(6), 1134-1143.

3. Ashok, S., Raj, S.M., Rathnasingh, C., Park, S., 2011. Development of recombinant *Klebsiella pneumoniae* Δ*dhaT* strain for the co-production of 3-hydroxypropionic acid and 1,3-propanediol from glycerol. Appl. Microbiol. Biotechnol. **90**(4), 1253-1265.

4. Cabelli, V., 1955. The tricarboxylic acid cycle in the oxidative and synthetic metabolism of *Klebsiella pneumoniae*. J. Bacteriol. 70(1), 23-29.

5. Celińska, E., 2012. *Klebsiella spp* as a 1, 3-propanediol producer: the metabolic engineering approach. Crit. Rev. Biotechnol. **32**(3), 274-288.

6. Celińska, E., 2010. Debottlenecking the 1,3-propanediol pathway by metabolic engineering. Biotechnol. Adv. **28**(4), 519-530.

7. Celińska, E., Grajek, W., 2009. Biotechnological production of 2,3-butanediol--current state and prospects. Biotechnol. Adv. **27**(6), 715-725.

460 8. Durgapal, M., Kumar, V., Yang, T.H., Lee, H.J., Seung, D., Park, S., 2014. Production of 1,3-
461 propanediol from glycerol using the newly isolated *Klebsiella pneumoniae* J2B. Bioresour.
462 Technol. **159**, 223-231.

463 9. Huang, Y., Li, Z., Shimizu, K., Ye, Q., 2012. Simultaneous production of 3-hydroxypropionic
464 acid and 1,3-propanediol from glycerol by a recombinant strain of *Klebsiella pneumoniae*.
465 Bioresour. Technol. **103**(1), 351-359.

466 10. Ji, X.J., Huang, H., Ouyang, P.K., 2011. Microbial 2,3-butanediol production: a state-of-the-
467 art review. Biotechnol. Adv. **29**(3), 351-364.

468 11. Kaur, G., Srivastava, A.K., Chand, S., 2012. Advances in biotechnological production of 1,3-
469 propanediol. Biochem. Eng. J. **64**(0), 106-118.

470 12. Kumar, V., Ashok, S., Park, S., 2013a. Recent advances in biological production of 3-
471 hydroxypropionic acid. Biotechnol. Adv. **31**(6), 945-961.

472 13. Kumar, V., Sankaranarayanan, M., Durgapal, M., Zhou, S., Ko, Y., Ashok, S., Sarkar, R., Park,
473 S., 2013b. Simultaneous production of 3-hydroxypropionic acid and 1,3-propanediol from
474 glycerol using resting cells of the lactate dehydrogenase-deficient recombinant *Klebsiella*
475 *pneumoniae* overexpressing an aldehyde dehydrogenase. Bioresour. Technol. **135**, 555-563.

476 14. Kumar, V., Sankaranarayanan, M., Jae, K.E., Durgapal, M., Ashok, S., Ko, Y., Sarkar, R., Park,
477 S., 2012. Co-production of 3-hydroxypropionic acid and 1,3-propanediol from glycerol
478 using resting cells of recombinant *Klebsiella pneumoniae* J2B strain overexpressing
479 aldehyde dehydrogenase. Appl. Microbiol. Biotechnol. **96**(2), 373-383.

480 16. Link, A.J., Phillips, D., Church, G.M., 1997. Methods for generating precise deletions and
481 insertions in the genome of wild-type *Escherichia coli*: application to open reading frame
482 characterization. J. Bacteriol. **179**(20), 6228-6237.

483 17. Maervoet, V.E.T., De Mey, M., Beauprez, J., De Maeseneire, S., Soetaert, W.K., 2011.
484 Enhancing the Microbial Conversion of Glycerol to 1,3-Propanediol Using Metabolic
485 Engineering. Org. Process Res. Dev. **15**(1), 189-202.

486 18. Mazumdar, S., Blankschien, M.D., Clomburg, J.M., Gonzalez, R., 2013. Efficient synthesis
487 of L-lactic acid from glycerol by metabolically engineered *Escherichia coli*. Microb. Cell
488 Fact. 12:7.

489 19. Oh, B.R., Seo, J.W., Heo, S.Y., Hong, W.K., Luo, L.H., Kim, S., Park, D.H., Kim, C.H., 2012.
490 Optimization of culture conditions for 1,3-propanediol production from glycerol using a
491 mutant strain of *Klebsiella pneumoniae*. Appl. Biochem. Biotechnol. **166**(1), 127-137.

492 20. Raj, S.M., Rathnasingh, C., Jo, J.-E., Park, S., 2008. Production of 3-hydroxypropionic acid
493 from glycerol by a novel recombinant *Escherichia coli* BL21 strain. Process Biochem.
494 **43**(12), 1440-1446.

495 21. Saxena, R.K., Anand, P., Saran, S., Isar, J., 2009. Microbial production of 1,3-propanediol:
496 Recent developments and emerging opportunities. Biotechnol. Adv. **27**(6), 895-913.

497 22. Wang, Y., Tao, F., Xu, P., 2014. Glycerol dehydrogenase plays a dual role in glycerol
498 metabolism and 2,3-butanediol formation in *Klebsiella pneumoniae*. J. Biol. Chem. 289(9),
499 6080-6090.

500 23. Wu, Z., Wang, Z., Wang, G., Tan, T., 2013. Improved 1,3-propanediol production by
501 engineering the 2,3-butanediol and formic acid pathways in integrative recombinant
502 *Klebsiella pneumoniae*. J. Biotechnol. **168**(2), 194-200.

503 24. Xu, Y.Z., Guo, N.N., Zheng, Z.M., Ou, X.J., Liu, H.J., Liu, D.H., 2009. Metabolism in 1,3-
504 propanediol fed-batch fermentation by a D-lactate deficient mutant of *Klebsiella*
505 *pneumoniae*. Biotechnol. Bioeng. **104**(5), 965-972.

506 25. Zeng, A.P., Biebl, H., 2002. Bulk chemicals from biotechnology: the case of 1,3-propanediol
507 production and the new trends. Adv. Biochem. Eng./Biotechnol. 74, 239–259.

508 26. Zheng, P., Wereath, K., Sun, J., van den Heuvel, J., Zeng, A.P., 2006. Overexpression of genes
509 of the DHA regulon and its effects on cell growth, glycerol fermentation to 1, 3-propanediol
510 and plasmid stability in *Klebsiella pneumoniae*. Process Biochem. 41(10), 2160-2169.

511

512

513

514 **Figure legends**

515 **Fig. 1** Flask culture of *K. pneumoniae* J2B Δ*ldhA*Δ*budO* with 29 mM (low) or 100 mM (high)
516 phosphate (Pi) in presence or absence of BDO (25 mM) and/or $NaHCO_3$ (100 mM). **A** and **B** 29
517 mM Pi; **C** and **D**, 100 mM Pi; **E** and **F,** 100 mM Pi with BDO; **G** and **H**, 100 mM Pi with
518 $NaHCO_3$; **I** and **J**, 100 mM Pi with BDO and $NaHCO_3$.

519 **Symbols:** In **A, C, E, G** and **I**, *filled triangle down* (residual glycerol), *half-filled circle* (cell
520 OD), *empty circle* (PDO), and *cross* (pH); in **B, D, F, H** and **J**, *empty squares* (ethanol), *empty*
521 *diamond* (acetate), *filled circle* (pyruvate), *filled triangle up* (formate), *empty circle* (BDO), *filled*
522 *star* (succinate), and *empty triangle up* (lactate).

523 **Fig. 2** Bioreactor culture of *K. pneumoniae* J2B Δ*ldhA* and Δ*ldhA*Δ*budO* with or without
524 continuous purging of CO_2 (0.05 vvm) or addition of $NaHCO_3$ (100 mM). **A** and **B**, Δ*ldhA*; **C**
525 and **D**, Δ*ldhA*Δ*budO*; **E** and **F**, Δ*ldhA*Δ*budO* with CO_2 purging; **G** and **H**, Δ*ldhA*Δ*budO* with
526 $NaHCO_3$.

527 **Symbols:** In **A, C, E**, and **G**, filled triangle down (glycerol), half-filled circle (cell OD), and
528 empty circle (PDO); in **B, D, F,** and **H**, *empty squares* (ethanol), *empty diamond* (acetate), *filled*
529 *circle* (pyruvate), *filled triangle up* (formate), *empty circle* (BDO), *filled star* (succinate), and
530 *empty triangle up* (lactate).

531 **Fig. 3** Fed-batch bioreactor culture of *K. pneumoniae* J2B Δ*ldhA* and Δ*ldhA*Δ*budO*. **A** and **B**,
532 Δ*ldhA* with 1 g/L yeast extract; **C** and **D**, Δ*ldhA*Δ*budO* with 1 g/L yeast extract; **E** and **F**,
533 Δ*ldhA*Δ*budO* with 5 g/L yeast extract.

534 **Symbols:** In **A, C,** and **E**, *filled triangle down* (glycerol), *half-filled circle* (cell OD), and *empty*
535 *circle* (PDO); in **B, D,** and **F**, *empty squares* (ethanol), *empty diamond* (acetate), *filled circle*
536 (pyruvate), *filled triangle up* (formate), *empty circle* (BDO), *filled star* (succinate), and *empty*
537 *triangle up* (lactate).

538 **Fig. 4** Glycerol dehydratase (DhaB) enzyme activity in presence of dihydroxyacetone (DHA),
539 dihydroxyacetone phosphate (DHAP), glyceraldehyde 3-phosphate (G3P), methylglyoxyl (MG)
540 and pyruvate.

Supplementary Fig. 1 Glycerol metabolism in *K. pneumoniae*. The genes encoding the relevant enzymes are shown in italics on the arrows. The encircled genes had been deleted in the current study. The solid lines represent single steps in the metabolic pathway, while broken lines indicate multiple steps (Ashok et al. 2011; Mazumdar et al. 2013).

Fig. 1

Buffer capacity	Low	High	High	High	High
2,3-BDO or Bicarbonate addition	None	None	2,3-BDO	Bicarbonate	2,3-BDO + Bicarbonate

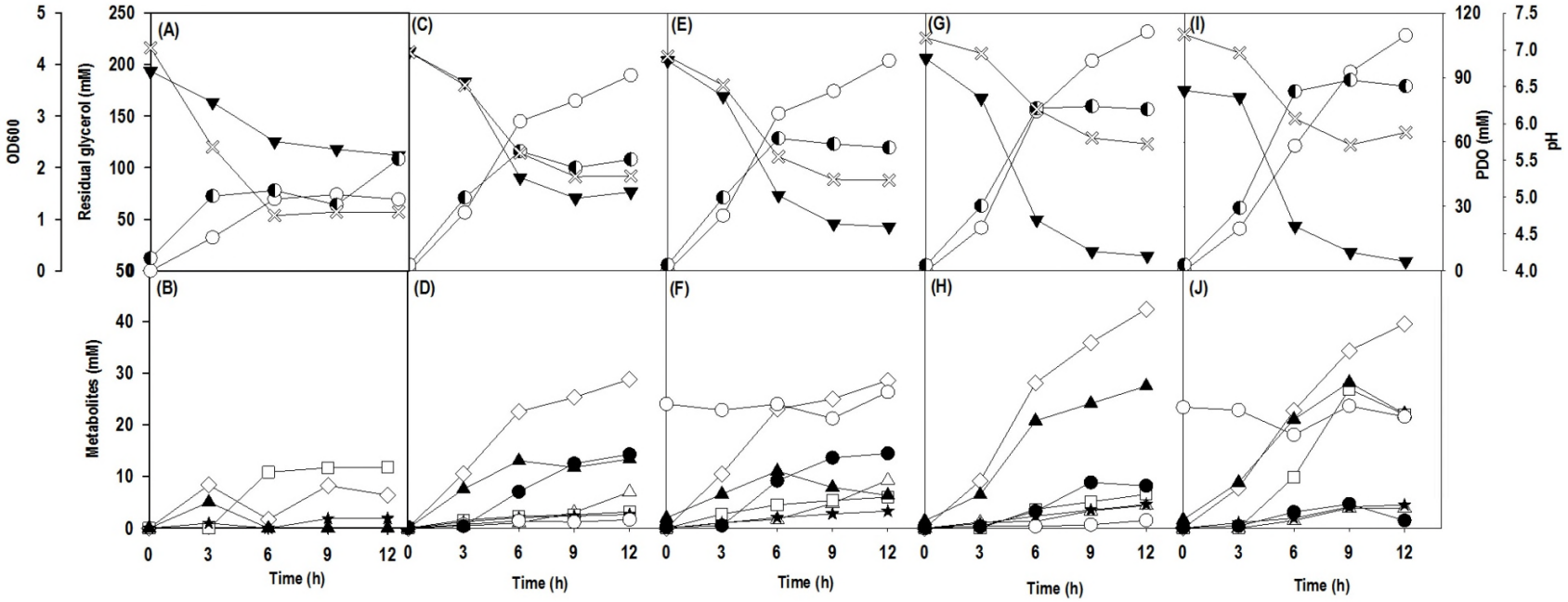

Fig. 2

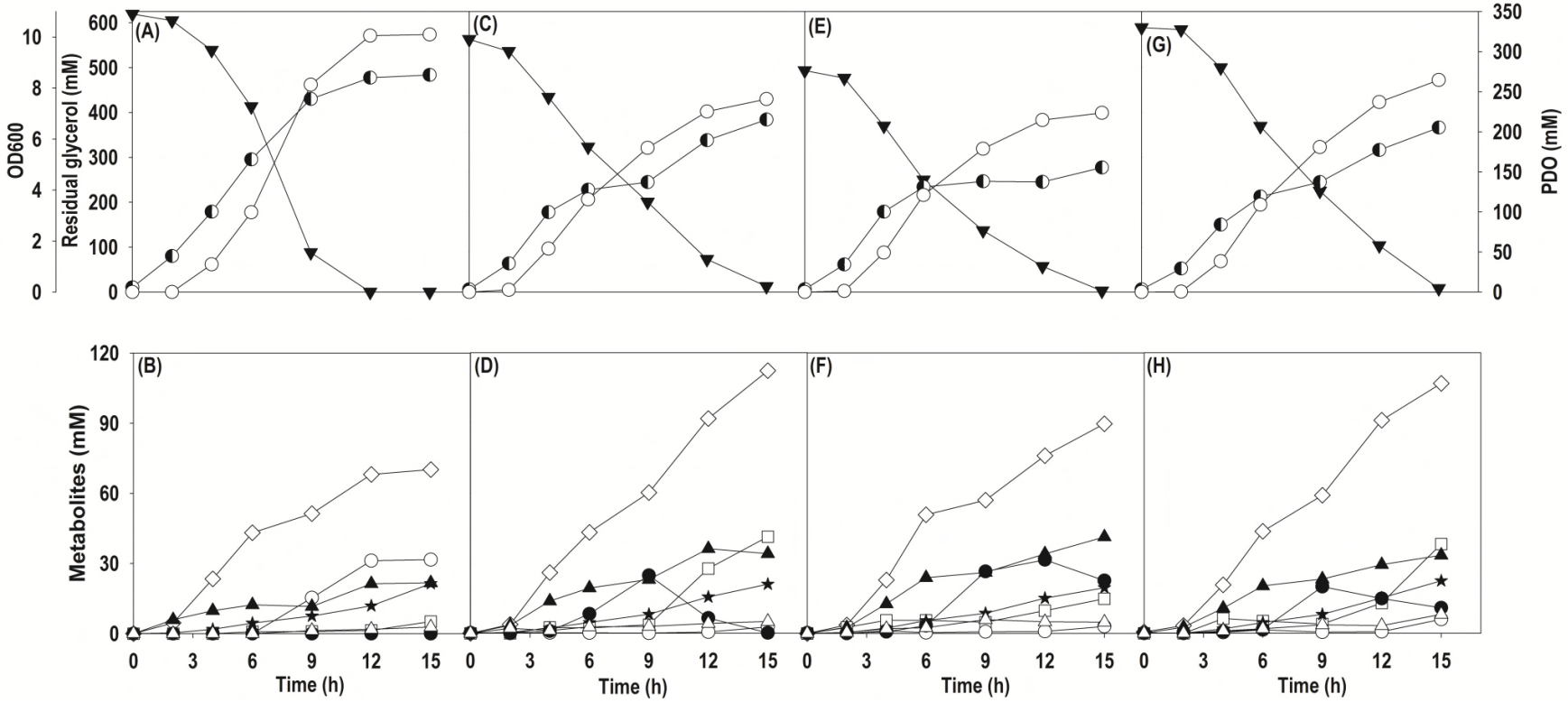
(A)
(C)
(E)
(G)
(B)
(D)
(F)
(H)
OD600
Residual glycerol (mM)
PDO (mM)
Metabolites (mM)
Time (h)
Time (h)
Time (h)
Time (h)

Fig. 3

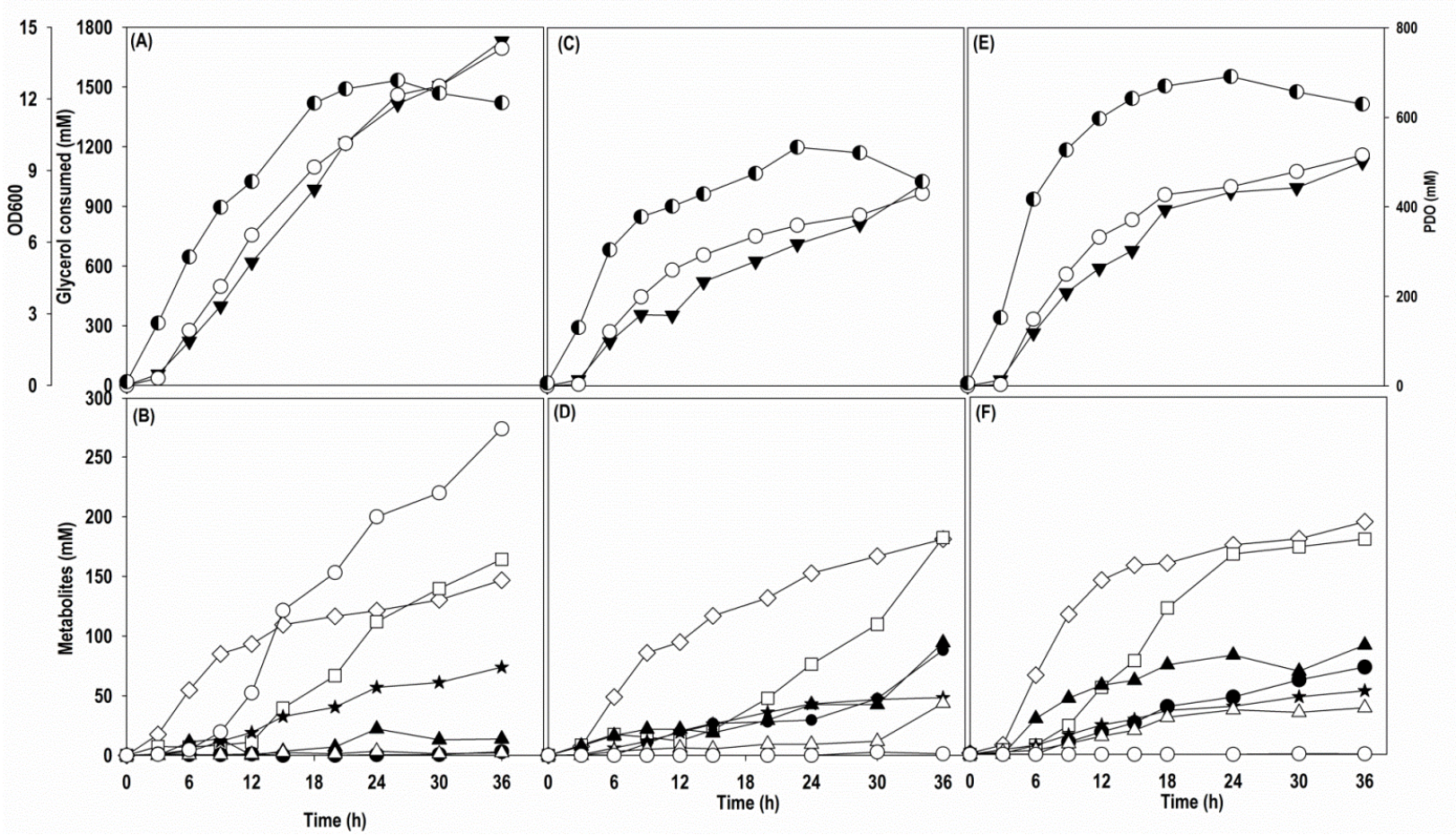
(A)
(B)
(C)
(D)
(E)
(F)
OD600
Glycerol consumed (mM)
Metabolites (mM)
PDO (mM)
Time (h)
Time (h)
Time (h)

Fig. 4

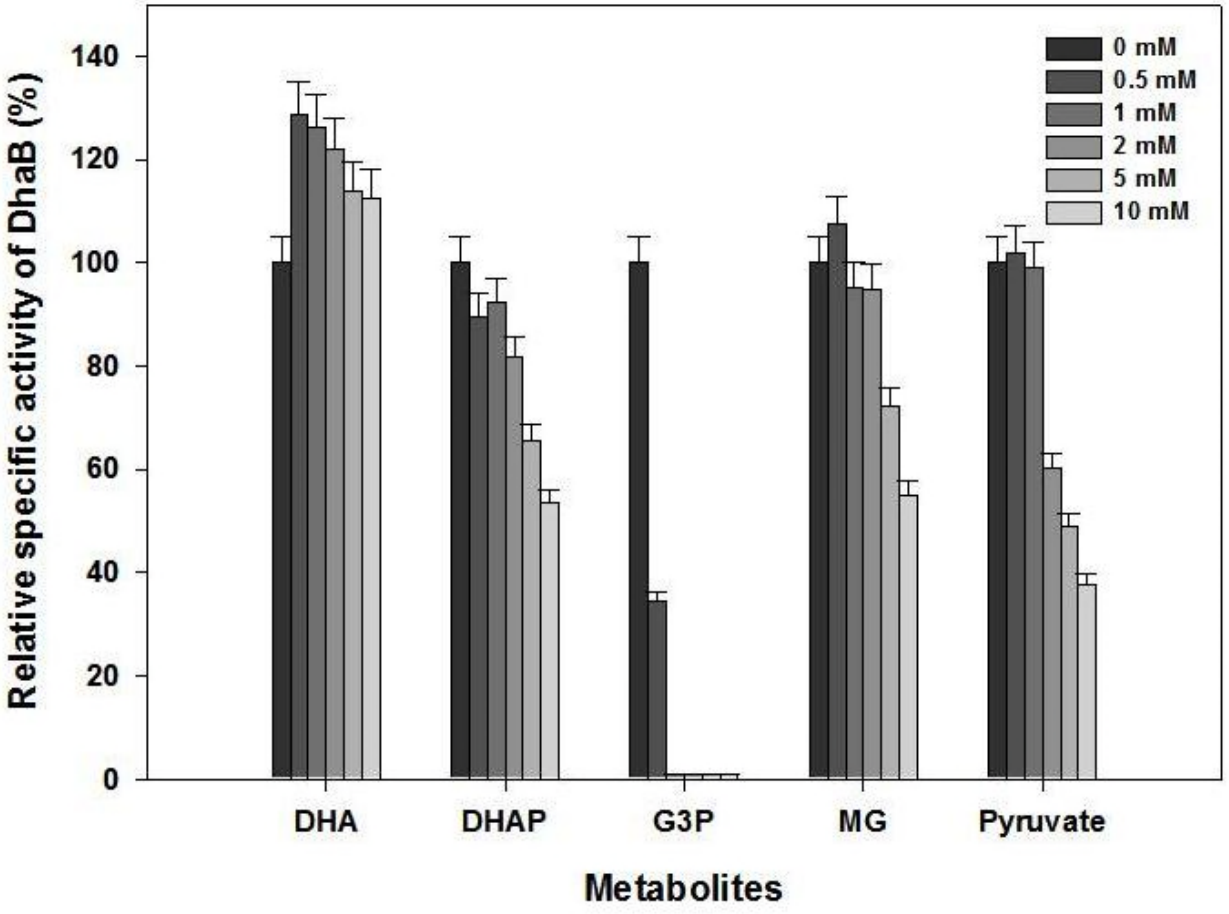
Relative specific activity of DhaB (%)
140
120
100
80
60
40
20
0
0 mM
0.5 mM
1 mM
2 mM
5 mM
10 mM
DHA
DHAP
G3P
MG
Pyruvate
Metabolites

Supplementary Fig. 1